Microwave Engineering
Ulm University

universität
uulm

Multi Target Simulator for Automotive Radar Sensors with Unknown Chirp-Sequence Modulation

Pirmin Schoeder, Benedikt Schweizer, Alexander Grathwohl, and Christian Waldschmidt

DOI: 10.1109/LMWC.2021.3088882

Multi Target Simulator for Automotive Radar Sensors with Unknown Chirp-Sequence Modulation

Pirmin Schoeder, *Graduate Student Member, IEEE*, Benedikt Schweizer, *Graduate Student Member, IEEE*, Alexander Grathwohl, *Graduate Student Member, IEEE*, and Christian Waldschmidt, *Senior Member, IEEE*

***Abstract*—In order to test and verify radar based systems for advanced driver assistance systems (ADAS), radar target simulators offer a test environment for reproducible dynamic automotive scenarios. This article presents a system capable of generating multiple targets with individual ranges and velocities for chirp-sequence frequency modulated continuous waveform (CS-FMCW) radars. The novel approach allows to generate targets without prior knowledge about the radar sensor by estimating the radar's waveform parameters. The proposed simulator offers high flexibility at low costs by performing the estimation on undersampled data. Finally, an automotive scenario of a spacially extended target is simulated for a radar sensor with the proposed system.**

***Index Terms*—automotive radar, chirp estimation, chirp-sequence, FMCW radar, radar target simulator.**

I. Introduction

The shift towards autonomous driving in the automotive industry creates the need for accurate and robust sensors to perceive precisely the surrounding environment of the vehicle. Radar sensors are therefore used to detect obstacles and other road users [1], [2]. The verification and characterization of increasingly complex ADAS, used to fulfill the high demands for autonomous functionality, is crucial. For validating and testing new features and radar systems, reproducible and flexible test scenarios are required. Radar target simulators offer a controllable environment for this set of requirements. To create realistic scenarios, a target simulator should be able to simulate several targets with individual ranges and velocities. Different architectures for the simulation of radar targets with variable range exist. The signal can be delayed digitally [3] [4] or by transmission lines [5] [6]. The combination of analog and digital delays has also been proposed [7]. Those systems realize the velocities of the targets by a frequency shift of the radar signal. A more flexible architecture, which is used for this target simulator as well, is a purely modulation-based simulator [8]–[11].

CS-FMCW radars allow the generation of ranges and velocities via modulation, since the evaluation of the time delay in the channel is measured indirectly via a frequency shift instead of measuring the time delay of the channel directly. The advantage of modulating the transmit signal, compared to delaying it, is that the amount of unique targets with given range and velocity is not limited by the system architecture. While a true time delay has to be realized digitally or via a transmission line for each individual range, modulating the superposition of multiple individual monofrequent target signals does not increase the system complexity [9], [10]. Additionally, ranges that are closer to the radar than the simulator itself can be created, whereas a negative time delay is non-causal and therefore impossible to be realized by delay-based architectures. To determine the required frequency of the modulating signal, the knowledge of the modulation parameters of the radar is needed, namely the slope of the frequency ramp S and the ramp repetition frequency $1/T_\mathrm{C}$. Compared to [8]–[10], where the modulation parameters were regarded as known, the presented target simulator is independent of a priori information, as the modulation parameters are estimated based on the first transmitted frequency ramps. In section II, the system concept is introduced, afterwards in section III the parameter estimation process is described. Lastly in section IV measurement results are presented.

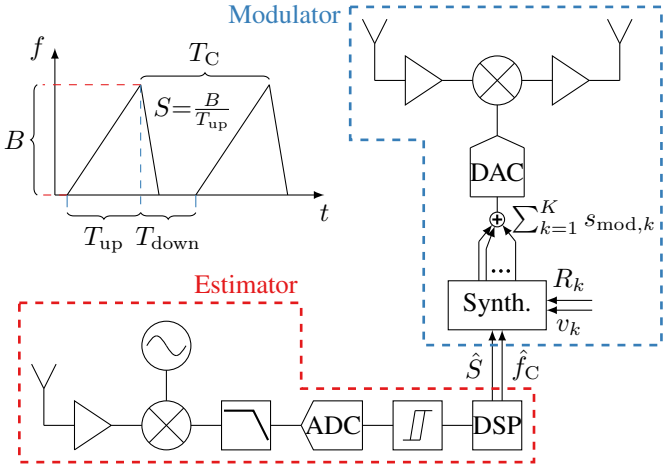

Fig. 1. Block diagram of the proposed system. The parameters of the chirp-sequence waveform are depicted in the upper left corner.

II. System Concept

The CS-FMCW waveform and the block diagram of the system is shown in Fig. 1. The system, consisting of the modulator and the estimator, is described in the following.

A. Modulator

The modulator's task is the generation of radar targets. In order to generate a target the transmit signal of the radar

Manuscript received May 04, 2021; revised June 01, 2021. This work was supported by the German Federal Ministry of Education and Research within the project SecForCARs. (Corresponding author: *Pirmin Schoeder*.)
The authors are with the Institute of Microwave Engineering, Ulm University, 89081 Ulm, Germany (e-mail: pirmin.schoeder@uni-ulm.de)

is received by an antenna, modulated by the mixer, and transmitted back to the radar. The transmit signal of the radar is modulated by an IQ-mixer in the RF domain. Amplifiers compensate for losses of the mixer and increase the amplitude for simulated targets with a high radar cross section (RCS). The synthesizer calculates the frequency $f_{\mathrm{mod},k}$ for all K targets, and synthesizes the sinusodial waveforms $s_{\mathrm{mod},k}$. The modulating signal, consisting out of the superimposed sinusodials, is generated with a digital-to-analog converter (DAC). Since the synthesis of the modulating signal is done in the digital domain, the RCS of the individual targets can be adjusted by a proportional factor. As shown in [10], a target with the Doppler shift f_{D} and the distance R can be generated by modulating the carrier of the radar chirp with a frequency f_{mod} of

$$f_{\mathrm{mod}} = \frac{1}{T_{\mathrm{C}}} \left\lfloor \frac{2RST_{\mathrm{C}}}{c_0} \right\rceil + f_{\mathrm{D}} \,, \tag{1}$$

where $\lfloor \cdot \rceil$ denotes rounding to the nearest integer, S is the slope of the frequency ramp, and T_{C} is the chirp repetition period. Therefore, the estimator needs to estimate T_{C} and S.

B. Estimator

The estimator converts the transmit signal of the radar into the complex baseband by IQ-mixing. After lowpass filtering the transmit signal of the radar is sampled. Finally, the ramp slope and the ramp repetition frequency are estimated. Since the absolute bandwidth B of a radar can be higher than 1 GHz to achieve a sufficient range resolution, sampling the entire bandwidth with the Nyquist rate would require analog-to-digital converters (ADC) with high sampling rates, leading to high hardware costs. To reduce the costs the estimation is performed on undersampled data. Therefore, the lowpass filter of the estimator does not act as an antialiasing filter, but its purpose is to reject unwanted products of the mixing stage and to filter out out-of-band noise. To further decrease the computational complexity, a trigger is implemented in field programmable gate array (FPGA) hardware that is able to detect whether a chirp was received. Only if the trigger detects a frequency ramp, the samples are saved in the system memory, and the estimation is performed in software with digital signal processing (DSP). Once the estimation is carried out, the modulation frequencies $f_{\mathrm{mod},k}$ can be updated.

III. Signal Model

A. Slope Extraction and Estimation

A frequency ramp sampled by the ADC of the estimator with a sampling rate of f_{s} can be modelled as a time-discrete complex chirp in the form

$$x(n) = A \exp\left(\mathrm{j}2\pi \left(\frac{S}{2f_{\mathrm{s}}^2} n + f_0 \right) n + \phi_0 \right) + \epsilon(n) \,, \tag{2}$$

where $\epsilon(n)$ is complex white gaussian noise with zero mean. The time-discrete samples are denoted as n. Following the scheme presented in [12], the estimated slope $\hat{S}\,(n)$ of the chirp can be extracted via

$$\frac{2\pi \hat{S}(n)}{f_{\mathrm{s}}^2} = \arg\big(x(n)\, x^*(n-1)\, x^*(n-1)\, x(n-2) \big) \,. \tag{3}$$

Multiplying the chirp with a time shifted version of itself leads to a compression. The maximum frequency slope is therefore restricted by the Nyquist limit of the sampling frequency:

$$S_{\max} \frac{1}{f_{\mathrm{s}}} \leq \frac{f_{\mathrm{s}}}{2} \Rightarrow S_{\max} \leq \frac{f_{\mathrm{s}}^2}{2} \,. \tag{4}$$

Because the chirp sequence waveform employs two chirps, the up- and downramp, and the possiblity of having a higher bandwidth than the lowpass filter of the estimator permits, the time samples of the up-ramp, used by the radar for the data aquisition, need to be extracted first. Once the chirp exceeds the analog bandwidth and noise dominates $x(n)$, taking the argument in (3) will create uncorrelated, uniformly distributed noise in the interval $[-\pi, \pi)$. Thus, the presence of a chirp can be detected by a low variance.

B. Chirp Repetition Period

The repetition period of the CS-FMCW waveform T_{C} can be estimated via the autocorrelation function (ACF). Since a constant starting point of the chirps cannot be guaranteed, the ACF of $x(n)$ will not yield reliable results, because the starting frequency f_0 in (2) can vary strongly due to the undersampling. However, the frequency modulation x_{FM}

$$x_{\mathrm{FM}}(n) = x(n)\, x^*(n-1) \tag{5}$$

is independent of the starting phase of the chirps, and f_0 of the chirp turns into a phase offset, leading to reliable results. The unbiased ACF of x_{FM} is defined as

$$\Psi_{zz}(m) = \frac{1}{N - |m|} \sum_{n}^{N} x_{\mathrm{FM}}(n)\, {x_{\mathrm{FM}}}^*(n-m) \,. \tag{6}$$

The number of samples between two distinct local maxima yields the information of the chirp repetition period T_{C}.

C. Estimation Error Analysis

The estimation of the chirp repetition rate $\hat{f}_{\mathrm{C}}$ will have an error of Δf_{C} compared to the true value:

$$\hat{f}_{\mathrm{C}} = f_{\mathrm{C}} + \Delta f_{\mathrm{C}} \,. \tag{7}$$

As can be seen in (1), the range of a target is created by the undersampling of f_{mod} with f_{C} by the factor of N_{us}:

$$N_{\mathrm{us}} = \left\lfloor \frac{2R\hat{S}}{c_0 \hat{f}_{\mathrm{C}}} \right\rceil \,. \tag{8}$$

Because N_{us} is multiplied with $\hat{f}_{\mathrm{C}}$ to create a target at range R with a velocity of zero, the velocity error due to an estimation error in $\hat{f}_{\mathrm{C}}$ will create an error in velocity:

$$f_{\mathrm{mod},v=0} = N_{\mathrm{us}} \hat{f}_{\mathrm{C}} = N_{\mathrm{us}} f_{\mathrm{C}} + N_{\mathrm{us}} \Delta f_{\mathrm{C}} \,. \tag{9}$$

If the velocity error Δv should be lower than $\Delta v_{\max}$, the error of the estimation should fulfill

$$|\Delta f_{\mathrm{C}}| \leq \frac{2f_0}{c_0 N_{\mathrm{us}}}\ \Delta v_{\max} < \frac{2f_0}{4R_{\max}B} \Delta v_{\max} \tag{10}$$

assuming that $T_{\mathrm{down}} < T_{\mathrm{up}}$.
As can be seen from (8), the error in range also scales with the

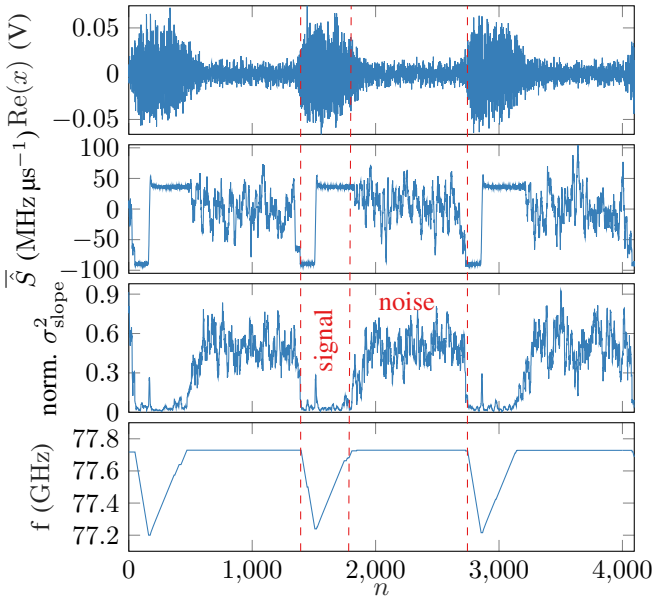

Fig. 2. Real part of the sampled signal (top), sliding mean (second) and normalized sliding variance (third) of the extracted slope, and the integrated slope within the bandwith of the system (bottom).

simulated range and the estimation error ΔS ($\hat{S}$=S+ΔS). If the maximum range error $\Delta R_{\max}$ should be smaller than the range resolution, the relative estimation error has to satisfy

$$\left|\frac{\Delta R_{\max}}{R_{\max}}\right| = \left|\frac{\Delta S}{S}\right| \leq \frac{c_0}{2BR_{\max}} \,. \tag{11}$$

IV. Measurements

For evaluating the performance of the proposed system, measurements on a CS-FMCW radar were performed. The bandwidth of the radar is 1.8 GHz between 77.2 GHz and 79 GHz with an upramp time T_{up}=50.025 µs and a downramp time T_{down}=20.025 µs, resulting in a chirp repetiton period T_{C}=70.05 µs. The estimator uses a lowpass filter with a cutoff frequency of 400 MHz, hence, only a fraction of the entire chirp bandwidth is sampled by the ADC. The sample rate f_{s} of the ADC is 19.231 MHz. When the FPGA chirp trigger detects a chirp waveform, 10^5 samples of the waveform are saved, and the estimation is performed in software.

A. Slope Estimation

In Fig. 2 the real part of the sampled signal is shown with the sliding mean $\overline{\hat{S}}$ and variance of the slope σ^2_{slope}. A high amplitude corresponds to a constant slope with a low variance. In case only noise is sampled, the variance of the estimated slope increases by an order of magnitude. By integrating the slope values with a normalized variance lower than 0.1, the chirp waveform can be recreated. After discarding the noisy samples and averaging the samples of the upchirp, a slope of 36.0114 MHz µs^{-1} is estimated compared to 35.982 MHz µs^{-1} that is expected by the settings of the radar. The relative error is 0.08 %, resulting in $R_{\max}$=102 m according to (11) with a maximum error of $\Delta R_{\max}$=0.08 m.

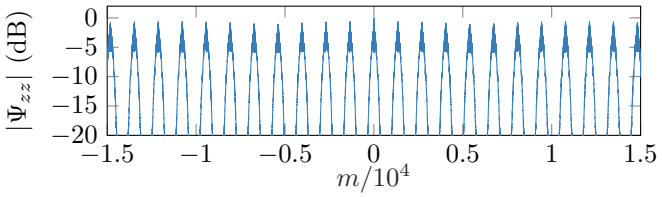

Fig. 3. ACF of the frequency modulation $x_{\text{FM}}(n)$ for estimating the ramp repetition frequency f_{C}.

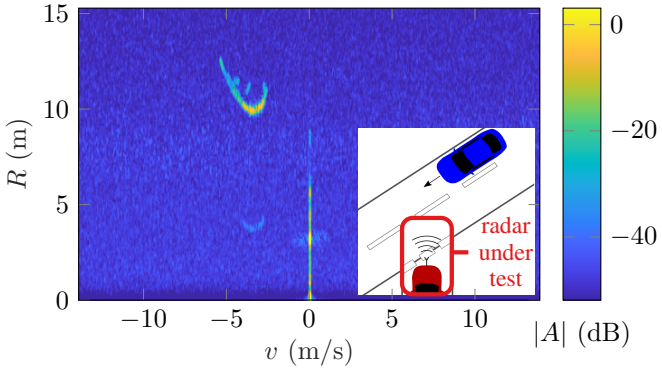

Fig. 4. Processed range-Doppler-plot of the automotive scenario, created by the target simulator. In the lower right corner a symbolic representation of the simulated scenario is depicted.

B. Chirp Repetition Period Estimation

Due to the recorded signal duration of 10^5 samples, the ACF is evaluated over 69 frequency ramps. A section of the ACF is shown in Fig. 3. The local maxima show whenever two chirps are overlapping after a shift of m. The evaluated difference in samples between two local maxima changes between 1347 and 1348, because the actual value lies between those two figures. The arithmetic mean over 69 ramps yields a time period of 70.0508 µs resulting in a relative error of 11.4 ppm and consequently a maximum velocity error of 0.545 m s^{-1} at $R_{\max}$=102 m (N_{us}=1715).

C. Target Simulation

The system was used to simulate an automotive scenario of a car approaching laterally the radar under test. The simulated car is represented by 90 point scatterers, modelled according to [13], to create an extended target. In Fig. 4 the resulting range-Doppler-plot of the scenario is depicted. The ghost target at R=4 m, v= − 4 m s^{-1} is caused by the limited side band suppression of 30 dB.

V. Conclusion

A radar target simulator was presented that directly modulates the carrier signal of a CS-FMCW radar sensor. By estimating the frequency slope and the chirp repetition frequency of the waveform, targets with arbitrary range and velocity information can be generated. By detecting the chirp waveform in hardware and extracting the needed parameters in software, a cost effective system architecture was developed that does not require a priori knowledge to generate targets with the designated velocity and range information.

REFERENCES

[1] F. Roos, J. Bechter, C. Knill, B. Schweizer, and C. Waldschmidt, "Radar sensors for autonomous driving: Modulation schemes and interference mitigation," *IEEE Microw. Mag.*, vol. 20, no. 9, pp. 58–72, 2019.

[2] N. Kern, M. Steiner, R. Lorenzin, and C. Waldschmidt, "Robust Doppler-based gesture recognition with incoherent automotive radar sensor networks," *IEEE Sens. Lett.*, vol. 4, no. 11, pp. 1–4, 2020.

[3] T. Dallmann, J. Mende, and S. Wald, "Atrium: A radar target simulator for complex traffic scenarios," in *IEEE MTT-S Int. Conf. on Microw. for Intell. Mobility (ICMIM)*, 2018, pp. 1–4.

[4] J. Sobotka and J. Novak, "Digital vehicle radar sensor target simulation," in *IEEE Int. Instrum. and Meas. Technol. Conf. (I2MTC)*, 2020, pp. 1–5.

[5] S. Lutz, C. Erhart, T. Walter, and R. Weigel, "Target simulator concept for chirp modulated 77 ghz automotive radar sensors," in *Eur. Radar Conf. (EuRAD)*, 2014, pp. 65–68.

[6] M. Engelhardt, F. Pfeiffer, and E. Biebl, "A high bandwidth radar target simulator for automotive radar sensors," in *Eur. Radar Conf. (EuRAD)*, 2016, pp. 245–248.

[7] A. Gruber, M. Gadringer, H. Schreiber, D. Amschl, W. Bösch, S. Metzner, and H. Pflügl, "Highly scalable radar target simulator for autonomous driving test beds," in *Eur. Radar Conf. (EURAD)*, 2017, pp. 147–150.

[8] W. Scheiblhofer, R. Feger, A. Haderer, and A. Stelzer, "Concept and realization of a low-cost multi-target simulator for CW and FMCW radar system calibration and testing," *Int. J. of Microw. and Wireless Technologies*, vol. 10, no. 2, pp. 207–215, 2018.

[9] F. Rafieinia and K. Haghighi, "ASGARD1: A novel frequency-based automotive radar target simulator," in *IEEE MTT-S Int. Conf. on Microw. for Intell. Mobility (ICMIM)*, 2020, pp. 1–4.

[10] J. Iberle, P. Rippl, and T. Walter, "A near-range radar target simulator for automotive radar generating targets of vulnerable road users," *IEEE Microw. and Wireless Compon. Lett.*, vol. 30, no. 12, pp. 1213–1216, 2020.

[11] F. Rafieinia and K. Haghighi, "System for generating virtual radar signatures," U.S. Patent 10,520,586, Dec. 31, 2019.

[12] P. M. Djuric and S. M. Kay, "Parameter estimation of chirp signals," *IEEE Trans. on Acoust., Speech, and Signal Process.*, vol. 38, no. 12, pp. 2118–2126, 1990.

[13] K. Schuler, D. Becker, and W. Wiesbeck, "Extraction of virtual scattering centers of vehicles by ray-tracing simulations," *IEEE Trans. on Antennas and Propag.*, vol. 56, no. 11, pp. 3543–3551, 2008.